Published in final edited form as:
Exp Brain Res. 2010 April ; 202(1): 213–229. doi:10.1007/s00221-009-2128-3.

Prehension synergies and control with referent hand configurations

Mark L. Latash,
Department of Kinesiology, The Pennsylvania State University, Rec.Hall-267, University Park, PA 16802, USA

Jason Friedman,
Department of Kinesiology, The Pennsylvania State University, Rec.Hall-267, University Park, PA 16802, USA

Sun Wook Kim,
Department of Kinesiology, The Pennsylvania State University, Rec.Hall-267, University Park, PA 16802, USA

Anatol G. Feldman, and
Department of Physiology, Centre for Interdisciplinary Research in Rehabilitation, University of Montreal, Montreal, QC, Canada

Vladimir M. Zatsiorsky
Department of Kinesiology, The Pennsylvania State University, Rec.Hall-267, University Park, PA 16802, USA

Mark L. Latash: mll11@psu.edu

Abstract

We used the framework of the equilibrium-point hypothesis (in its updated form based on the notion of referent configuration) to investigate the multi-digit synergies at two levels of a hypothetical hierarchy involved in prehensile actions. Synergies were analyzed at the thumb–virtual finger (VF) level (VF is an imaginary digit with the mechanical action equivalent to that of the four actual fingers) and at the individual finger level. The subjects performed very quick vertical movements of a handle into a target. A load could be attached off-center to provide a pronation or supination torque. In a few trials, the handle was unexpectedly fixed to the table and the digits slipped off the sensors. In such trials, the hand stopped at a higher vertical position and rotated into pronation or supination depending on the expected torque. The aperture showed non-monotonic changes with a large, fast decrease and further increase, ending up with a smaller distance between the thumb and the fingers as compared to unperturbed trials. Multi-digit synergies were quantified using indices of co-variation between digit forces and moments of force across unperturbed trials. Prior to the lifting action, high synergy indices were observed at the individual finger level while modest indices were observed at the thumb–VF level. During the lifting action, the synergies at the individual finger level disappeared while the synergy indices became higher at the thumb–VF level. The results support the basic premise that, within a given task, setting a referent configuration may be described with a few referent values of variables that influence the equilibrium state, to which the system is attracted. Moreover, the referent configuration hypothesis can help interpret the data related to the trade-off between synergies at different hierarchical levels.

Correspondence to: Mark L. Latash, mll11@psu.edu.

Keywords

Prehension; Synergy; Referent configuration; Grip

Introduction

Recent developments of the equilibrium-point hypothesis to the control of multi-effector and whole-body movements have resulted in the concept of referent configuration (RC; reviewed in Feldman and Levin 2009). RC is a configuration at which all the involved muscles would have achieved zero activation levels, while any deviations from RC lead to changes in muscle activation. Therefore, RC may also be addressed as threshold body configuration. Actual equilibrium body configurations commonly deviate from RC because of external forces (including gravity) and/or constraints that may be imposed by external objects (such as rigid obstacles preventing motion of body parts) and the body anatomy.

Prehensile tasks have been commonly described in terms of digit forces (reviewed in Johansson 1996; Zatsiorsky and Latash 2008), that is kinetic variables. In a recent study, Pilon and colleagues (2007) have shown that motion of a hand-held object, associated with anticipatory adjustment of grip force, can result from changes in a component of the referent body configuration—the referent arm-hand configuration. In this framework, the normal force during prehension emerges following the difference between the referent aperture between the opposing digits and the actual aperture constrained by the size of the object between the digits. The purpose of this study is to develop this view, test some of its predictions, and link the RC hypothesis with the idea of multi-digit prehension synergies.

Consider a five-digit prismatic grasp where all the points of digit contact with the hand-held object are in one plane (the grasp plane); an external torque acts in the same plane, i.e. the torque vector is normal to the plane (Fig. 1). Such a task has been analyzed as a two-level hierarchy (Arbib et al. 1985;Iberall 1987;Santello and Soechting 2000;Zatsiorsky and Latash 2008;Latash and Zatsiorsky 2009). At the upper level, the task is shared between the thumb and a virtual finger (VF, an imagined digit with the mechanical action equal to the combined action of all four fingers). At the lower level, the VF action is shared among the four fingers. Consider the task at the upper level. Holding an object statically imposes four constraints. First the resultant normal force should be zero. Second, the resultant tangential force should be equal in magnitude to the object weight and directed against the force of gravity (load, L). Third, the resultant moment of force should be equal in magnitude and directed against the external moment of force (M). Fourth, the normal forces should be sufficient to prevent object slippage at the given friction conditions.

We assume that the control of this action may be described with a small set of referent variables. Such a set may include referent aperture (AP_{REF}, centered about a point AP_{CTR}; cf. Pilon et al. 2007), referent position in the vertical direction (Z_{REF}), and referent orientation of the object with respect to the vertical (α_{REF}).

Note that setting any AP_{REF} smaller than the actual aperture leads to a discrepancy between the referent and actual digit tip coordinates in the horizontal direction. This discrepancy results in active muscle force production trying to move the digits towards their respective referent coordinates. If the thumb and VF normal forces are not equal, i.e. if AP_{CTR} does not coincide with the midpoint between the opposing digits, the object will move in a horizontal direction until the two forces are balanced thus satisfying the first of the four mentioned constraints. Setting a referent vertical coordinate Z_{REF} will similarly lead to balancing the external load with the sum of the thumb and VF vertical forces, while setting α_{REF} allows to balance the moment of force for the required orientation of the object (vertical in Fig. 1).

Using the described mode of control defines, given certain external conditions, characteristics of the overall action of the hand on the object such as grip (normal) force, total load resisting force, and total moment of force. It does not define unambiguously, however, contributions of the individual digits (for example, the thumb and VF forces) to the overall hand action. Across repetitive trials, the digit forces and moments of force may be expected to co-vary, as long as they do not lead to major changes in the resultant force and moment of force acting on the object. Such co-varied changes in elemental variables (forces and moments of force produced by individual digits) that keep important characteristics of the overall hand action unchanged have been addressed as prehension synergies (Santello and Soechting 2000; Zatsiorsky and Latash 2004, 2008).

Several recent studies produced quantitative estimates of prehension synergies at the two introduced levels (Gorniak et al. 2007a, b, 2009). In these studies, an index of synergy was computed reflecting the amount of co-variation among elemental variables across repetitive trials that helped stabilize the mechanical output at that particular level. High synergy indices at the upper level were accompanied by low synergy indices at the lower level suggesting a conflict between synergies at the two levels.

In this study, we test several predictions of the suggested two-level hierarchical scheme and control with RC for an experiment when the subject plans to move a hand-held object quickly and the object unexpectedly happens not to be in the hand. First, we predict that such an unexpected unloading of the hand would lead to a new configuration of the hand and digits compatible with the idea of unchanged referent variables such as AP_{REF}, Z_{REF}, and α_{REF}. The unloading will lead to a decrease in the external forces acting on the hand, and the hand will move towards the referent coordinates (assuming that the subject does not react to the perturbation, that is, does not interfere with the natural hand movement, cf. Feldman 1966; Latash 1994). In particular, in the unexpectedly unloaded ('empty-hand') trials, we predict non-monotonic changes in the aperture between the thumb and the opposing digits, i.e. the digits moving towards each other and then away from each other. This prediction is based on the documented transient increase in the grip force in the middle of such actions related to the expected inertial forces (Flanagan et al. 1999, 2006; Gysin et al. 2003). We expect the hand to move to a higher vertical location similarly to the classical results in experiments with arm unloading (Feldman 1966). We also expect the hand to rotate in the direction opposite to the external torque created by the unbalanced load attached to the object.

Second, we expect to see strong synergies at the upper level of the hierarchy during the unperturbed lifting actions while synergies at the lower level may be present or absent (as in Gorniak et al. 2009).

Third, if the subject is asked to produce a certain, low magnitude of the grasping force prior to lifting the object, this task may be associated with setting not AP_{REF} but referent coordinates for each of the opposing sets of digits (the thumb and the set of four fingers comprising the VF). Setting a referent VF coordinate defines VF normal force while it allows finger forces to co-vary as long as VF force corresponds to the difference between the referent and actual VF tip coordinates. Hence, we expect to see a synergy at the lower level stabilizing the VF normal force (in contrast to the second prediction). During this phase, there may or may not be a synergy at the upper level of the hierarchy stabilizing the resultant horizontal force acting on the object since keeping the resultant force at zero (or any other value) is not part of the task.

Methods

Subjects

Ten healthy right-handed university students (five males and five females) participated in this experiment. Subjects were all right-handed according to their hand usage during eating and writing. Their mean (±SD) anthropometric characteristics were: age 27.7 ± 5.5 years, weight 68.1 ± 13.1 kg, height 170 ± 8.2 cm, hand width 7.5 ± 0.9 cm, and hand length 17.5 ± 1.2 cm. Each participant's hand length was measured between the middle fingertip and the distal crease of the wrist with the hand extended, and their hand width was measured between the lateral aspect of the index and little finger metacarpophalangeal (MCP) joints. None of the subjects had a history of neurological or peripheral disorders of the hand or professional training that might affect their hand function, such as playing musical instruments. All subjects gave informed consent according to the procedures approved by the Office for Research Protection of the Pennsylvania State University.

Apparatus

A customized aluminum handle was attached to the top edge of an aluminum beam (4.5 × 16 × 0.6 cm) at the midpoint of the beam in the medio-lateral direction; the handle and beam apparatus created an inverse T shape (Fig. 2a). Five six-component (three forces and three torques) transducers (four Nano-17s and one Nano-25, ATI Industrial Automation, Gerner, NC, USA) were mounted on the aluminum handle. The transducers measured the forces and moments of force applied by the fingers (Nano-17) and by the thumb (Nano-25). The moments are recorded-with respect to the centers of the contact area of the sensors.

Four motion capture ProReflex cameras (Model MUC 240, Qualisys) recorded the three-dimensional coordinates of the passive markers at a sampling frequency of 240 Hz. The cameras were placed 1.0–1.5 m from the table, on which the subject's hand and handle were placed. The system was calibrated before data collection for each subject. The system calibration yielded less than 0.25 mm error within a working area of 100 × 100 × 60 cm (Fig. 2c). Each marker coordinate was represented in a global coordinate system (X^k, Y^k, Z^k). The center of mass of the unloaded handle was determined by suspending the handle at different points. Two loads (0.21 kg) were fixed either symmetrically at the endpoints (zero external torque condition) or there was only one load attached to the left or right endpoint. When the load was placed at the left endpoint, it required a supination effort to keep the handle vertical (SU condition). When the load was placed at the right endpoint, it required a pronation effort (PR condition). The magnitude of the external torque was 0.15 Nm.

The force/torque sensors were evenly distributed, 20 mm between their centers, and the thumb sensor was placed opposite the midpoint between the middle and ring fingers. Hence, the center points of the sensors were 30 mm above (index finger), 10 mm above (middle finger), 10 mm below (ring finger), and 30 mm below (little finger) the midpoint (0 mm), about which the thumb sensor was centered. The sensors were aligned in the Y–Z plane (see Fig. 2). The grip width, defined as the shortest distance between the contact surfaces of the thumb and finger sensors in the horizontal direction, was 86 mm. The plane containing the centers of all five sensors will be referred to as the grasp plane.

Smooth nylon pads were placed on the round contact surface of each sensor in order to decrease the friction between the digits and the transducers. To measure the static friction coefficient (μ) between the skin and the nylon pad, the subjects were asked to grasp the handle with the thumb and index finger and then decrease the grasping force as slowly as possible. Slips were detected by a sudden decrease in the tangential force at the thumb and index fingers. The friction coefficient was computed as the ratio between the normal force and the tangential force at slip (Johansson and Westling 1984, Aoki et al. 2006). The friction coefficient (μ) was 0.6 ± 0.07.

A locking system was attached to the bottom of the handle, and a hole was made in the table top such that the loop of the locking system was directly under the table top when the handle rested on the table vertically (Fig. 2a). In the locked state, a metal rod (3 cm diameter) was passed through the eyehook under the table such that the subject could not see it. The total weight of the handle, beam, transducers, and two loads was 9.1 N.

The output analog signals from the sensors (6 components × 5 sensors) were fed into the 12-bit analog–digital converter (PCI-6031, National Instrument, Austin, TX, USA) and were processed and saved by a customized LabVIEW program (LabVIEW 8.1, National Instrument, Austin, TX, USA) on a desktop computer (Dell Dimension 8200, Austin, TX, USA). The 3D coordinates of the markers were recorded and identified with the Qualisys Track Manager (Qualisys, Gothenburg, Sweden) on another desktop computer (Dell Dimension 8300, Austin, TX, USA). A customized LabView program was used for data acquisition, and Matlab programs were written for data processing.

Experimental procedure

The subjects cleaned and dried their hands to normalize the skin condition. Before testing, the subjects were given an orientation session that explained the apparatus and the procedure to ensure that they were able to accomplish the task properly. Light-weight spherical retro-reflective markers (3 mm in diameter) were attached to the dorsal aspect of hand. Due to limitations in the experimental setup, data were recorded only from the thumb, index and little fingers. For these three digits, markers were adhered to consistently identifiable and palpable surface landmarks: to the center of each fingernail, to the three joints of each digit, to the radial and ulnar styloids, and to the midpoint between the two wrist markers (a total of 15 markers, see Fig. 2d). We used the fingertip markers to track the position of the handle during the task. Finger flexion and extension, abduction and adduction, and hand pronation and supination movements were calculated from the motion capture data.

During the experiment, the subject sat on a chair, faced the testing table and rested his/her elbow and wrist on the table with his/her upper arm at approximately 45° abduction in the frontal plane and his/her forearm at approximately 135° flexion in the sagittal plane. The forearm was supinated 90°; thus, the hand was positioned in a natural grasping position. The handle was placed on the table and aligned with the right shoulder of subject. The subject was requested to place his/her forearm in a starting position prior to each trial (Fig. 2c). The starting forearm position was identified by a drawing on a board and defined by the size of each subject's forearm, but his/her forearm was not constrained by any physical means. In the starting position, the fingers were close to, but not touching, the sensors as the subject prepared to grip the inverse T-shaped handle.

During the testing, the computer generated a warning beep (alerting subjects to get ready), and a yellow cursor showing the total normal force produced by all four fingers (I, M, R, and L) started to move along the screen. The subjects were asked to statically grasp the handle and match their total finger normal force with the horizontal line (10 N) shown on the monitor. This force was much smaller than typical forces generated during the object motion (see Fig. 5; "Results"). The second time interval, which started after the trial initiation, was shown as a thick dotted vertical line. At any time within this interval, the subjects were asked to lift the handle up rapidly to match a visually presented target (20 cm from the top of the handle) in a self-paced manner and then hold the handle naturally and statically in the air until they heard a beep at the end of the trial. There were no explicit accuracy constraints; the subjects were asked to consider the target only as an approximate point showing them where to stop. Note that after the handle started to move, the monitor stopped giving feedback about the level of force. Two practice trials were given prior to each condition. The subjects were instructed to perform the movement in a single stroke and not to attempt to correct the ongoing movement even if it happened to be inaccurate. The three torque conditions (zero torque, PR effort, and SU effort) were presented as blocks in a balanced order across the subjects.

In perturbed trials, the handle was locked under the table using the invisible rod (Fig. 1). The rod could be moved to lock the handle without any perceptible vibrations; we interviewed the subjects after the experiment, and they all admitted that they had been unable to predict whether the handle had been locked or not. When the handle was locked, the digits slipped off the sensors and the hand moved upwards, while the handle stayed on the table. The digits moved into flexion in perturbed trials, but they never touched one another in any of the trials. The subjects were instructed not to correct their hand motion in cases of perturbations. We told them "to let the hand move the way it naturally does," i.e., not to correct hand movements if the fingers slipped off the handle because it was stuck on the table. Each block consisted of fifteen unperturbed trials, followed by six trials where each trial was randomly selected to be perturbed or unperturbed. As there were three torque conditions, there were a total of 63 trials. The order of the blocks was randomized and balanced across subjects. There were 1-min intervals between trials and at least 5-min intervals between the conditions. The total duration of each experiment was about 1.5 h.

Data analysis

Customized data acquisition software written in LabVIEW was used to convert the digital signals into force and moment values. For kinematic data processing, each of the markers was identified and tracked in the Qualisys Track Manger. In some of the trials, some of the markers were occluded or merged with other markers. Missing markers in the intervals before and after the lifting movements were interpolated for portions of the path that showed 20 or less missing points (100 ms). During the movement, trials were discarded if there were more than 10 points (50 ms) missing. On average, three trials were discarded per subject.

Both kinetic and kinematic measurements were digitally low-pass filtered with a second-order, zero-lag Butterworth filter at 20 Hz. For each accepted trial, the onset of the voluntary action was identified using the thumb normal finger force. The time of action initiation (t_0) was defined as the time when the time derivative of the thumb normal force reached 5% of its peak level for that trial. All trials were aligned by t_0 for further analysis. Note that t_0 was calculated from the force data rather than the position data, because the increase in grip force preceded the handle movement.

The kinetic and kinematic data processing was performed using Matlab. Three time intervals were identified within each action:

1. The "constant force phase" was the period of time when the fingers produced about 10 N before the lifting movement was initiated (before t_0).
2. The "lifting phase" was defined as the period between the onset of the movement (t_0) and the time of peak height (H_{PEAK}) computed as the height when the average tangential velocity of the wrist markers crossed zero after reaching the peak velocity.
3. The "holding phase" was defined as the last 1 s of the movement.

Kinematic analysis

The vertical movement distance (D_Z) was defined as the height reached, after the movement was complete, by the thumb marker as measured by the cameras (in the Z^k direction in the lab-fixed reference system). In the unperturbed conditions, D_Z was close to the target height (20 cm). For perturbed conditions, D_Z could vary substantially. The difference (ΔD_Z) between D_Z in a perturbed trial and its averaged value in unperturbed trials was computed for each perturbed trial. Positive values of ΔD_Z indicate that in the perturbed condition, the hand was higher than in the unperturbed condition.

Grip aperture (W) was defined as the minimal distance between the thumb and the line connecting the centers of the index and little finger sensors. This distance was unchanged in unperturbed trials because of the constraints imposed by the handle, 94 ± 3 mm across subjects; it differs from the handle width because the sensors were placed on the top of the fingernails. The aperture could change in the perturbed trials as a function of time. For each perturbed trial, the change in grip aperture, ΔW was defined as the difference between the constant aperture in the unperturbed trials and the minimum value of $W(t)$ in that trial. Positive values of ΔW indicate that the aperture was smaller in the perturbed condition.

Rotation of the line connecting the carpometacarpal (CMC) and MCP joint markers was described using Euler angles, with the $X - Y' - Z''$ sequence (Zatsiorsky 1998). Hand rotation was defined as the maximum rotation about the X axis in this decomposition. The change in hand rotation ($\Delta\theta$) between perturbed and unperturbed trials was defined as the difference between the maximal hand rotation in a perturbed trial and in the averaged unperturbed trials. The hand rotations in the counterclockwise direction (pronation) were designated as positive.

Kinetic analysis

The forces of the individual force sensors were first transformed into the coordinate system of the handle. In the transducer-fixed reference system, the normal force F_i^n (where the subscript i refers to individual digits) corresponds to the Z-direction. In the initial position, F_i^n was oriented horizontally with respect to the global coordinate system. The Y-axis of each transducer was aligned with the vertical axis. The force along the Y-axis will be referred to as tangential force, F_i^t.

The normal and tangential forces of the individual digits, VF, and the resultant force can be represented as:

$$\begin{bmatrix} F^n_{\mathrm{VF}} \\ F^t_{\mathrm{VF}} \end{bmatrix} = \begin{bmatrix} \sum_{i=1}^{4} F_i^n \\ \sum_{i=1}^{4} F_i^t \end{bmatrix}, \quad i=\{\mathrm{I, M, R, L}\} \tag{1}$$

$$\begin{bmatrix} F^n_{\mathrm{TOT}} \\ F^t_{\mathrm{TOT}} \end{bmatrix} = \begin{bmatrix} \sum_{j=1}^{5} F_j^n \\ \sum_{j=1}^{5} F_j^t \end{bmatrix}, \quad j=\{\mathrm{I, M, R, L, T}\} \tag{2}$$

where I, index; M, middle; R, ring; L, little; and T, thumb. The resultant (subscript "TOT") normal force of the five digits was expected to be close to zero, while the resultant tangential force of the five digits was expected to be close to the load when the handle was not moving.

Since each finger makes soft finger contact with the sensor surface (Mason and Salisbury 1985), the digits could roll on and push against the sensor surfaces, but they could not pull on

NIH-PA Author Manuscript

NIH-PA Author Manuscript

the sensors. The position of the point of normal digit force application with respect to the sensor center (the center of pressure, CoP) was calculated as $CoP_X = -m_Y/F_Z$ and $CoP_Y = m_X/F_Z$, where CoP stands for the center of pressure; m_X and m_Y signify the moments of force about the local *X*- and *Y*-axis with respect to the center of the sensor surface. The moments of individual finger forces and the resultant moment acting on the handle about the *X*-axis passing through the center of the handle were calculated:

$$M^j = d_Y^j \cdot F_Z^j - d_Z^j \cdot F_Y^j \quad (3)$$

$$M = \sum_j M^j \quad (4)$$

where *j* stands for all digits including the thumb *j* = (I, M, R, L, T), *F* is force, *d* is a moment arm, and *M* stands for moment of force about the *x*-axis. Upward tangential forces and counterclockwise moments (PR moments) were defined as positive. In the text, moments of force exerted by the subjects, not produced by external loads are presented.

Analysis of force and moment-of-force stabilizing synergies—The purpose of this analysis was to compute indices of covariation of elemental variables (forces and moments of force) produced by sets of effectors that reflect the stabilization of combined effector outputs. This analysis was performed at two levels: the individual finger (lower) level and the VF–thumb (upper) level. Note that at the upper level, four constraints of statics have to be satisfied to keep the object motionless in the hand:

$$0 = F_{VF}^n + F_T^n \quad (5)$$

$$-L = F_{VF}^t + F_T^t \quad (6)$$

$$-M = \underbrace{F_T^n d_T + F_{VF}^n d_{VF}}_{\text{Moment of the normal forces} \equiv M^n} + \underbrace{F_T^t r_T + F_{VF}^t r_{VF}}_{\text{Moment of the tangential forces} \equiv M^t} \quad (7)$$

$$kF_{VF}^n > F_{VF}^t ; kF_T^n > F_T^t \quad (8)$$

where the superscripts refer to normal (*n*) and tangential (*t*) forces, *d* and r are moment arms of the normal and tangential forces respectively, and *k* is a friction coefficient.

At the lower level, co-variation of elemental variables produced by individual fingers was studied, while at the upper level, co-variation of elemental variables produced by the VF and the thumb was studied. The index of covariation was computed as the difference between the sum of the variances of elemental variables [ΣVar(*EV*)] and the variance of the total output of these elemental variables [Var(Σ*EV*)]. According to the Bienaymé theorem (Loeve 1955), for independently varying variables, the two values should be equal to each other. Hence positive values of the index corresponded to predominantly negative co-variation among the elemental variables, which we interpret as stabilization of their combined output.

For each condition and subject, there were at least 12 acceptable unperturbed trials. Hence, exactly 12 trials were chosen for each condition and each subject for this analysis. These trials were aligned by the moment of action initiation (t_0). The VF normal force was computed as the sum of the magnitudes of the four finger normal forces at each time sample. The time profiles of the variances of each individual digit normal force (Var$F_j(t)$, j = I, M, R, L, T), the VF normal force [Var$F_{VF}(t)$], and the total normal force [Var$F_{TOT}(t)$] were computed across the trials at each point in time for each condition and subject separately. The time profile of the sum of the variances of the individual finger normal forces, ΣVar$F_j(t)$, was also computed. Further, an index of force co-variation at the lower and higher levels were computed as:

$$\Delta V_{F,\mathrm{IF}}(t) = \left[\sum \mathrm{Var}F_j(t) - \mathrm{Var}F_{\mathrm{VF}}(t)\right] / \sum \mathrm{Var}F_j(t) \quad (9)$$

$$\Delta V_{F,\mathrm{HAND}}(t) = \left[\mathrm{Var}F_{\mathrm{VF}}(t) + \mathrm{Var}F_T(t) - \mathrm{Var}F_{\mathrm{TOT}}(t)\right] / \left[\mathrm{Var}F_{\mathrm{VF}}(t) + \mathrm{Var}F_T(t)\right] \quad (10)$$

Likewise, indices for moment of force co-variation at the two levels were computed as:

$$\Delta V_{M,\mathrm{IF}}(t) = \left[\sum \mathrm{Var}M_j(t) - \mathrm{Var}M_{\mathrm{VF}}(t)\right] / \sum \mathrm{Var}M_j(t) \quad (11)$$

$$\Delta V_{M,\mathrm{HAND}}(t) = \left[\mathrm{Var}M_{\mathrm{VF}}(t) + \mathrm{Var}M_T(t) - \mathrm{Var}M_{\mathrm{TOT}}(t)\right] / \left(\mathrm{Var}M_{\mathrm{VF}}(t) + \mathrm{Var}M_T(t)\right) \quad (12)$$

Note that $\Delta V > 0$ implies predominantly negative covariation among forces (or moments of force) produced by the individual digits. We interpret such values as signs of a force (or moment of force) stabilizing synergy (Gorniak et al. 2007a, b; Kang et al. 2004; Shim et al. 2005). Larger positive ΔV values correspond to larger amounts of negative co-variation, thus a stronger synergy. A result of $\Delta V = 0$ implies independent variation of digit forces (or moments of force), and correspondingly the absence of a synergy, while $\Delta V < 0$ may be interpreted as co-variation of elemental variables destabilizing their combined output. The normalization limits the value of ΔV indices by +1 for perfect force (or moment) stabilizing synergies (the individual elemental variables change their value in time but variance of the performance variable equals zero).

Analysis of apparent stiffness—We will use the term "apparent stiffness" (see Latash and Zatsiorsky 1993; Zatsiorsky 2002) defined as the change in force (or moment of force) per unit of linear displacement (or rotational displacement) imposed by a change in the external loading conditions. For simplicity, we assume linear relations between changes in displacements and forces (moments of force).

Previous studies of the apparent stiffness of the fingers (Kao et al. 1997; Hajian and Howe 1997; Milner and Franklin 1998) and of a grasping hand (van Doren 1998; Friedman and Flash 2007) used small perturbations of the fingers in order to calculate the stiffness matrices. In this study, a different approach was used. In the perturbed conditions, motion of the hand to a higher location, motion of the thumb and fingers towards each other, and rotation of the hand in pronation/supination was observed (see "Results"). During these perturbed trials, the fingers were no longer on the force sensors, and so it was not possible to measure the actual change of force corresponding to the change of hand posture. Rather, we assume that the final position corresponded to zero force applied by the fingers, and calculated the change of force from the average force that was applied in the same external torque condition in the unperturbed trials.

In particular, tangential apparent stiffness (K_T) was defined as the change of tangential force per unit of the change in the hand height: $\Delta F^{t}_{\mathrm{TOT}} = K_T\ (\Delta D_Z)$. Aperture apparent stiffness (K_A) was defined as a change in the normal VF force per unit of change in the aperture: $\Delta F^{n}_{\mathrm{TOT}} = K_A\ (\Delta W)$. Rotational apparent stiffness (K_R) was defined as the change of the moment of force about the handle-fixed *x*-axis per unit of change in the rotation of the hand: $\Delta M = K_R(\Delta\theta)$. All computations were performed between the individual perturbed trials and the averaged values across the unperturbed trials.

Statistical analysis

The data are presented in the text as means and standard errors of the mean. Mixed-effects ANOVA with the factors *Torque* (three levels: PR, ZERO, and SU), *Condition* (two levels: perturbed and unperturbed) and *Digit* (three levels: thumb, index, and little) were used.

To estimate the effects on the apparent stiffness indices K_A, K_T, and K_R, an ANOVA was run with the factors *Torque* (three levels: PR, ZERO, and SU).

For ΔV analysis, a three-way repeated measures ANOVA was run with the factors *Index* (two levels: ΔV_F and ΔV_M), *Level* (two levels: VF-TH and IMRL), and *Phase* (two levels: before and after the perturbation). The levels of the *Phase* factor were defined as the average over 500 ms of steady state before t_0 and after t_0 Appropriate pair-wise contrasts and post-hoc Tukey's Honestly Significant Difference (HSD) tests were used to further analyze significant effects of ANOVA. The level of significance was set at $p < 0.05$.

Results

Mechanics of the perturbed and non-perturbed movements

During the unobstructed lifting of the handle, the subjects showed nearly straight trajectories independently of the external torque. The initial and final hand positions are shown for a typical subject in Fig. 3a. When the object was fixed to the table (perturbed condition), the digits slipped off the sensors and the hand showed a much more curved trajectory. Figure 3b shows the initial and final hand postures for a typical perturbed trial (zero external torque condition). In the perturbed case, the vertical movement amplitude was always larger, and the fingers and the thumb moved towards each other such that the grip aperture decreased.

Time series of several kinematic variables are illustrated in Fig. 4 for the trials with zero external torque. The trials were aligned by the time of grip force increase (see "Methods") and then averaged across trials for a typical subject. Panel A illustrates the increase of height of the hand during the task, with the hand moving higher in the perturbed case. Panel B shows the approximately constant horizontal positions of the thumb and index finger for unperturbed movements, and the large changes in the perturbed case. Panel C shows an approximately bell-shaped vertical velocity profile in the unperturbed case, and a correction for an overshoot in the perturbed case. Panel D shows a decrease in the grip aperture during the perturbed trials (aperture is constant in the unperturbed case). Note that in the perturbed trials, the hand took longer to start moving because it had to overcome the friction between the digit tips and the sensors.

Statistical analysis has shown an increase in both the peak height of the hand (measured at the time of the largest overshoot) and the ultimate steady-state height in the unloaded trials. On average, the peak height increased from 0.25 ± 0.15 to 0.30 ± 0.2 m, while the steady-state height increased from 0.22 ± 0.09 to 0.24 ± 0.09 m. These differences have been confirmed by two-way ANOVAs, *Condition* (unobstructed vs. perturbed) × *Torque* (PR, ZERO, SU) that showed an effect of *Condition* ($F_{[1, 18]} > 5.71$; $p < 0.01$) without an effect of *Torque* and without an interaction.

The increase in movement amplitude was accompanied by an increase in the peak velocity (on average, from 1.79 ± 0.14 to 2.53 ± 0.24 m/s) and in the peak acceleration (on average, from 25.4 ± 2.5 to 73.0 ± 5.6 m/s^2). Both results have been confirmed by similar two-way ANOVAs that showed main effects of *Condition* ($F_{[1,18]} > 12.6$; $p < 0.001$) and *Torque* ($F_{[1,18]} > 57.8$; $p < 0.001$).

Maximal deviations of trajectories from a perfect vertical path more than doubled in the perturbed trials as compared to the unobstructed trials (10.4 ± 0.9 vs. 4.2 ± 0.4 cm). These deviations were also higher in the presence of a non-zero external torque as compared to those under zero external torque (on average, by 15 ± 4%). These results were confirmed by a two-way ANOVA that showed effects of both *Condition* ($F_{[1,18]} = 249.23$; $p < 0.001$) and *Torque* ($F_{[2,36]} = 2.95$; $p < 0.01$) without a significant interaction. Pair-wise comparisons confirmed larger deviations under the PR and SU torques as compared to zero torque ($p < 0.05$) without a difference between the PR and SU torques.

In unobstructed trials, the normal force (grip force) showed an increase simultaneously with the tangential force (load force). Typical time profiles of the two forces are shown in Fig. 5a and b. Note that the final steady-state value of the grip force is elevated as compared to the initial prescribed value of 10 N. In perturbed trials, the initial changes in the two forces followed closely those observed in the unobstructed trials (compare the thick and thin lines in Fig. 5a, b). After the digits slipped off the sensors, about 100 ms after the action initiation, both grip and load force data became zero.

The peak value of the grip (normal) force was smaller in the perturbed trials, on average by 15 ± 4% (Fig. 5c), while the peak value of the load (tangential) force was higher in the perturbed trials, on average nearly by 41 ± 3% (Fig. 5d). Both differences were significant according to the two-way ANOVA that showed significant effects of *Torque* ($F_{[2,36]} > 7.2$, $p < 0.01$) and *Condition* ($F_{[1,18]} > 15.41$, $p < 0.001$), without a significant interaction.

Apparent stiffness

The tangential apparent stiffness (K_T) was estimated as the ratio of the increase in the hand displacement (ΔD_Z) to the change in the tangential forces (ΔF^{t}_{TOT}) in the perturbed trials as compared to the unobstructed trials. These two quantities are plotted in Fig. 6a. They are both higher in the ZERO external torque condition compared to the PR and SU conditions, confirmed by an ANOVA, *Torque* × *Condition*. There was a significant effect of *Torque* on ΔD_z ($F_{[2,18]} = 3.86$, $p < 0.05$), and on $\Delta F^{t}_{\mathrm{TOT}}$ ($F_{[2,18]} = 20.32$, $p < 0.01$).

Across the external torque conditions, the K_T value was, on average, 3.33 ± 0.75 N/cm (PR 3.64 ± 0.75 N/cm; ZERO 3.01 ± 0.81 N/cm; SU 3.36 ± 0.71 N/cm). This value was significantly positive ($p < 0.01$; Wilcoxon's test). These values are comparable to those found for two-finger pinching in Kao et al. (1997): 2.99 N/cm, three finger pinch in Van Doren (1998): 4.82 N/cm, and for grasping a cup from the side in Friedman and Flash (2007): 6.52 N/cm.

Changes in the grip aperture (ΔW) in the perturbed trials were quantified using the distance between the thumb and the line joining the tips of the index and little fingers. Recall that in the unperturbed trials, the digit tips stayed on the sensors and the aperture remained constant—defined by the handle geometry. The grip aperture reduced from its initial value (prescribed by the handle width) to a minimum value before returning to a new steady state. If the thumb contacted one of the other digits, the aperture would be expected to dwell at the minimum for some time before moving to the new steady state. However, this was never observed.

In the perturbed trials, the minimum grip aperture was on average 7.1 ± 0.6 cm less than in the unperturbed case. This difference was significant as confirmed by an ANOVA, *Condition* × *Torque*, that showed main effect of both *Condition* ($F_{[1,18]} = 24.2$; $p < 0.001$) and *Torque* ($F_{[2,18]} = 3.75$; $p < 0.05$). The latter effect reflected the significantly larger ΔW under the SU condition as compared to the PR condition. There was no significant interaction.

After reaching the minima, the hand aperture increased to a magnitude that was, on average, 1.9 ± 2.6 cm less than in the unperturbed case. This difference was statistically significant according to a two-way ANOVA, *Condition* × *Torque*, which showed an effect of condition ($F_{[1,18]} = 5.5$, $p < 0.05$) without any other effects.

The apparent aperture stiffness (K_A) was estimated as the ratio of the decrease in the hand aperture (ΔW) to the grip forces $\Delta F^{n}_{\mathrm{TOT}}$ in the unperturbed trials. These two quantities are plotted in Fig. 6b. On average, K_A was 7.0 ± 0.7 N/cm; it did not depend on external torque.

When the external torque was zero, there was no difference in the magnitude of the hand rotation in the frontal plane between the unobstructed and perturbed trials, the average difference was less than 1°. When the torque was non-zero, however, unobstructed trials showed significant differences from the perturbed ones. In particular, when the subjects planned a movement against a SU load, they showed in the perturbed trials hand rotation into SU that was, on average, 13.8 ± 2.5°, as compared to the unobstructed trials. In contrast, under the PR load, the perturbed trials showed excessive hand rotation into PR that was, on average, 17.2 ± 2.6°, as compared to the unobstructed trials. There was a main effect of *Torque* ($F_{[2,18]} = 39.36$; $p < 0.001$) without other effects.

The apparent rotational stiffness of the hand (K_R) was estimated as the ratio of the change in the hand rotation ($\Delta\theta$) in the frontal plane to the moment about the *x*-axis (ΔM) applied by the fingers. These two quantities are plotted in Fig. 6c. As the change in hand rotation for the zero external torque case was close to zero, K_R was not calculated for this condition. The average magnitude of K_R for the other two conditions was 1.77 ± 0.28 Nm/rad. (PR 1.32 ± 0.25 N/cm; SU 2.22 ± 0.31 N/cm). This value was significantly positive ($p < 0.01$) and not different across the two torque conditions as confirmed by ANOVA.

Analysis of multi-digit synergies

We used two indices, $\Delta V_F(t)$ and $\Delta V_M(t)$, to assess effects of co-variation of individual digit forces and moments across trials on stabilization of the total grip force and total moment of force produced by the digits and acting on the handle. To remind, these indices represent the normalized difference between the sum of the variances in the space of elemental variable (individual digit forces/moments) and the variance in the performance variable (total force and total moment). Their positive values correspond to negative co-variation of elemental variables that stabilizes the performance variable. Such analyses were performed at the upper level (thumb and VF) and at the lower level (individual four fingers) of the assumed hierarchy (see “Introduction” and “Methods”).

When the subject gripped the handle on the table, both total grip force and total moment of force were stabilized by co-varied adjustments of finger forces and moments of force across trials. This was reflected in positive $\Delta V_F(t)$ and $\Delta V_M(t)$. At the initiation of the lifting action (t_0), the values of ΔV_F and ΔV_M both increased at the upper level and dropped at the lower level. As a result, at the new steady state, both the total grip force and the total moment of force were strongly stabilized at the upper level ($\Delta V > 0$), while they showed positive co-variation potentially destabilizing the output of the four fingers at the lower level ($\Delta V < 0$).

Figure 7 illustrates the time profiles $\Delta V_F(t)$ and $\Delta V_M(t)$ at the two levels over all three torque conditions. Note the similarity of the graphs for the PR, ZERO, and SU torques. Note the positive ΔV values prior to the action; on average, ΔV indices averaged over the 0.5 s interval during the first steady state were 0.72 ± 0.03 for ΔV_F at the upper level, 0.85 ± 0.03 for ΔV_F at the lower level, 0.28 ± 0.08 for ΔV_M at the upper level, and 0.38 ± 0.08 for ΔV_M at the lower level. After the action, at the upper level, ΔV_F averaged over 0.5 s increased to 0.91 ± 0.01 while ΔV_M increased to 0.63 ± 0.05. At the same time, at the lower level, ΔV_F dropped to −0.55 ± 0.15 while ΔV_M dropped to −0.63 ± 0.14.

These findings were supported by a three-way ANOVA that showed significant effects of all three factors, *Index* [$F_{(1,36)} = 20.92$; $p < 0.001$], *Level* [$F_{(1,36)} = 60.25$, $p < 0.001$], and *Phase* [$F_{(1,36)} = 43.82$, $p < 0.001$] and a significant *Level* × *Phase* interaction [$F_{(1, 36)} = 87.61$, $p < 0.001$]. The effect of *Index* reflected the overall higher values for ΔV_F than for ΔV_M. The effect of *Level* reflected the overall higher indices for the upper level as compared to the lower level.

Discussion

Our experiments confirmed the main predictions formulated in the Introduction. In the initial condition, before the lifting action, we observed strong force and moment of force stabilizing synergies at the lower level of the assumed hierarchy (i.e., at the level of four individual finger actions) corresponding to our third prediction. There were also force and moment of force stabilizing synergies at the higher level (i.e., at the level of thumb and VF actions). After the movement initiation, both synergies at the lower level disappeared, while the synergies at the upper level became stronger (as quantified by the ΔV index). These observations correspond to our second prediction. When the object was unexpectedly fixed to the table, the loading conditions changed, and we observed new configurations of the hand and digits reproducible across subjects. In particular, we observed non-monotonic pattern of changes in the grip aperture, and new values of the hand height, hand rotation in pronation–supination, and grip aperture at the final steady state. These observations confirm our first prediction. In the following sections, we discuss relationships of the results to the RC hypothesis and address the issue of synergies at different levels of a control hierarchy.

Moving towards the referent configuration

Two competing views exist on the neural control of voluntary movements by redundant systems. According to the first view, the central nervous system (CNS) uses internal models that predict and implement requisite forces moving the system from the initial state to a desired final state (reviewed in Wolpert et al. 1998; Shadmehr and Wise 2005). We will address this view as “force-control”. According to the alternative view, the CNS defines time profiles of neural variables, such as thresholds of activation of neuronal pools, while all the performance variables (including forces) emerge as a result of interactions among the neuromotor processes within the body and between the body and the external force field (Kugler and Turvey 1987; Feldman and Levin 1995; Latash 2008). Arguments in favor of or against these schemes have been published recently (Hinder and Milner 2003; Ostry and Feldman 2003; Feldman and Latash 2005; Feldman and Levin 2009).

In our experiment, the unexpected unloadings of the hand resulted in the finger tip forces becoming zero immediately after the fingers slipped of the sensors. The disappearance of the rigid walls of the handle was expected to lead to motion of the digit tips towards each other resulting in a new steady-state value of the grip aperture (see Pilon et al. 2007). However, we also observed a less trivial, reproducible non-monotonic pattern of changes in the grip aperture: The digits flexed and then extended. Although we did not record electromyographic signals (a shortcoming of the study), the extension motion of the digit was likely produced by activation of the extensor muscles. Within the framework of the RC hypothesis, this could happen if, in the unloaded trials, extensor muscles transiently became longer than their referent (threshold) length values for activation. Note that in the unperturbed trials, the walls of the object did not allow the digits to move and stretch the extensor muscles. As a result, their actual length was always shorter than the referent length and no major phasic activation was expected that could reverse the digit motion direction (here we ignore the relatively minor co-activation of extensors during typical lifting actions).

There is one more physiological reason for an unchanged time pattern of RC to lead to non-monotonic changes in the aperture in the unloaded trials: Sudden unloading of finger muscles may lead to a silent period in the flexor muscle spindle discharge, resulting in a temporal decrease in the flexor muscle activation and reversing the movement direction (especially in the low-inertial fingers). Indeed, a geometric consequence of using an unchanged RC pattern may be an unchanged (or only slightly changed) time pattern of referent aperture (AP_{REF} in Fig. 1). It has a minimum soon after the movement initiation corresponding to a transient peak in the grip force and then it settles at a new steady-state value (see Pilon et al. 2007). In the unloaded trials, actual aperture showed a non-monotonic time profile similar to that of AP_{REF}. To our knowledge, the flexion–extension pattern of digit motion, after the hand slipped off the sensors and moved up without the handle, would not be predicted by other hypotheses on grip force-control.

The other two features of hand motion were more predictable: The removal of the weight of the object reduced the gravitational load on the hand, and the hand was expected to move higher up, towards a new equilibrium position (closer to Z_{REF}, Fig. 1). This result is similar to the effects of unloading reported in several studies (Feldman 1966;Schmidt and McGown 1980;Latash and Gottlieb 1990). Along similar lines, the removal of the external torque (in the PR and SU conditions) was expected to lead to a new hand orientation in space (closer to α_{REF} Fig. 1). All these predictions were confirmed (see Figs. 3, 4, 5 and 6).

According to the RC-hypothesis, RC (a combination of activation thresholds for relevant neuronal pools) is reflected in a set of referent variables – coordinates, to which the effectors tend to move (see Fig. 1). It also leads to certain stability properties of the effectors about those coordinates (Feldman and Levin 1995,2009; cf. impedance control, Hogan 1985). We quantified this second component of RC using indices of apparent stiffness (Latash and Zatsiorsky 1993). The reproducible results across subjects suggest that these indices do reflect common features of control of such tasks.

These interpretations hinge on the mentioned assumption of non-intervention by the subjects. It is possible that, despite the instruction, the subjects showed triggered (preprogrammed) reactions that led, in particular, to the observed non-monotonic changes in the digit aperture (Traub et al. 1980; Johansson and Westling 1984). As shown in Fig. 4, the thumb and the fingers moved towards each other and reached a minimum of the aperture value soon after the movement initiation, and later the hand opened and reached a new steady-state aperture, smaller than the initial aperture value. We would like to note that pre-programmed reactions are known for their phasic nature and inconsistent amplitude if perturbations are unexpected (Marsden et al. 1981). In contrast, the steady-state new aperture values were consistent both within and across the subjects.

Synergies and control with referent configurations

Several recent studies explored motor synergies based on quantitative analysis of variance in kinetic, kinematic, and electromyographic spaces (reviewed in Latash et al. 2007). In a redundant system of elements, variance in the space of elemental variables may be viewed as consisting of two components defined with respect to a particular, potentially important performance variable produced by the system. One of the components does not affect the performance variable; it has been addressed as compensated, goal-equivalent, or, simply, “good” variance (V_{GOOD}). The other component leads to changes in the performance variables (uncompensated, non-goal-equivalent, or “bad”, V_{BAD}). Analysis of the two variance components has been developed within the uncontrolled manifold (UCM) hypothesis (Scholz and Schöner 1999; reviewed in Latash et al. 2002b), which assumes that the space of elemental variables is organized by the controller into two sub-spaces, compatible (UCM) and incompatible with a desired value of a performance variable.

The existence of the mentioned two variance components may be discussed within the RC hypothesis. First, it is possible that the controller facilitates a group of RCs that are consistent with the task demands and then, in each trial, randomly selects one RC from this set. Then, RC variability will result in a family of equivalent solutions for the motor task, i.e., in proportionally higher V_{GOOD} computed with respect to performance variables that are important within the task context.

Second, it is possible that a single RC specifies activation thresholds for neuronal pools that are reflected in higher-order variables such as, for example, referent aperture, while elemental variables (forces and moments of force) produced by elements (individual digits) are free to vary in a sub-space compatible with the referent aperture and external conditions (cf. Pilon et al. 2007). So, the existence of the two variance components is a natural consequence of choice of a RC (or RC set) that meets the task demand.

In our study (see the simple illustration in Fig. 1), potentially important performance variables were identified based on the task mechanics. Equations (5)–(8) in “Methods” reflect mechanical constraints for keeping the object perfectly vertical and perfectly motionless. Note, however, that these constraints could be (and very likely were) violated in experiments, for example, if the handle was slightly rotated or if the object trembled a bit. So, we expected to see, across trials, a certain amount of “bad” variance with respect to such variables as resultant horizontal force, total tangential (load resisting) force, and total moment of force. These constraints, however, are compatible with any amount of “good” variance. So, by themselves, they do not necessitate synergies (in a sense $V_{GOOD} > V_{BAD}$, see Latash et al. 2007).

Several studies have suggested that synergies may be seen in the absence of such explicit constraints, i.e. reflecting a preference by the controller that may not have an obvious mechanical interpretation (Latash et al. 2001; Niu et al. 2007). Moreover, sometimes synergies in similar tasks are seen in some subjects but not in others; they can also emerge in the process

NIH-PA Author Manuscript

NIH-PA Author Manuscript

of practice (Latash et al. 2002a; Kang et al. 2004; Scholz et al. 2003). These observations suggest that some of the synergies may be related to setting a referent value of a variable that is not easy to guess and that may not have a straightforward mechanical interpretation.

Imagine now that a similar grasping task is performed by two persons such that the opposing digits (thumb and VF) are controlled by different brains. In such a case, referent coordinates have to be set separately for the thumb and VF. This may or may not lead to their synergic adjustment (for example, based on afferent information) such that the equations of statics are satisfied. Indeed, a recent study has shown that two-person tasks may be associated with synergies similar to those seen in one-person tasks; however, these synergies showed lower covariation indices (Gorniak et al. 2009).

A recent series of studies have suggested that, in a hierarchically controlled system, synergies at different levels of the hierarchy may be in conflict with each other (Gorniak et al. 2007a, b, 2009). A strong synergy stabilizing a performance variable (for example, resultant horizontal force) at the upper (thumb–VF) level of a hierarchy means that $V_{\mathrm{GOOD}} > V_{\mathrm{BAD}}$. As such, large V_{GOOD} contributes to stronger synergies. Note, however, that both V_{GOOD} and V_{BAD} contribute to variance of each of the elemental variables at the higher level; in particular, large V_{GOOD} leads to high variance of the VF output. Consider now the lower level of the hierarchy. At that level, variance of the VF output, by definition, corresponds to V_{BAD}. So, large V_{GOOD} at the upper level leads to high V_{BAD} at the lower level.

In our experiment, prior to the action, the subjects were asked to produce a certain magnitude of the total normal force by the VF. This was expected to be accomplished by setting an adequate RC that produced a referent coordinate for the VF. Individual finger forces were expected to show synergies stabilizing the normal force of the VF as in earlier pressing tasks (Latash et al. 2002c; Gorniak et al. 2007b; Zhang et al. 2008). This was indeed observed. There was no specific requirement for the moment of force produced by the VF in the initial position. It is reasonable to assume that a natural, default action would correspond to zero net moment of force (cf. minimization of secondary torques, Zatsiorsky et al. 2000; Li et al. 2001; Zhang et al. 2009) associated with a corresponding referent orientation. Altogether, this control is expected to lead to strong synergies at the lower level stabilizing both VF force and moment of force. The thumb and VF actions are not coupled in the initial state; hence, no strong synergies are expected at the upper level.

The initiation of the lifting action is associated with a qualitative change in the control: The combined thumb–VF action has to satisfy task requirements, and the upper control level becomes leading. This was indeed associated with much stronger synergies stabilizing both force and moment of force at the upper level. At the same time, the synergies at the lower level disappeared as expected from the trade-off between synergies at the two hierarchical levels, as described earlier. Taken together, these observations support the earlier hypothesis on a trade-off between synergies at different hierarchical levels (Gorniak et al. 2007a, b).

Typical studies of multi-joint actions forming the basis of the force-control view involved movements by a kinematically non-redundant effector (typically, a two-joint system performing a two-dimensional task, e.g., Shadmehr and Mussa-Ivaldi 1994; Hinder and Milner 2003; Kluzik et al. 2008). As a result, the problem of motor redundancy and the associated issue of synergies have not been addressed within this line of studies. As shown in a recent study of multi-joint synergies in the process of practicing reaching movements in an unusual force field (Yang et al. 2007), such synergies show non-trivial changes involving increased self-motion (joint motion leading to no motion of the endpoint) that looks wasteful and meaningless within the force-control view. This study has shown limitations of the force-control ideas in handling natural movements by redundant systems of effectors. The interactions between synergies at the two hierarchical level demonstrated in our study can be addressed within the RC hypothesis, while such issues have been beyond the level of analysis within the force-control approach.

Concluding comments

The main goal of this study has been to explore how the concept of prehension synergy can be naturally incorporated into the idea of control with RC. Our observations are overall compatible with the basic premise that, within a given task, setting a RC may be described with a few referent variables that influence the equilibrium state to which the system is attracted. Moreover, the RC control can help interpret the data related to the trade-off between synergies at different hierarchical levels. Further controlled studies are necessary with mechanical perturbations applied to redundant motor systems (see Adamovich et al. 2001; Rossi et al. 2002). Unfortunately, so far, most perturbation studies with well controlled kinetics and kinematics have studied non-redundant motor tasks such as, for example, planar movements of two-joint systems (Shadmehr and Mussa-Ivaldi 1994). There are a few notable exceptions (e.g., Yang et al. 2007). However, most of those studies focused on processes of adaptation to perturbations rather than using perturbations to discover the nature of control variables and their task-specific patterns.

We have to admit several shortcomings of the current experimental design. First, we used only a few unexpectedly unloaded trials and could not track likely adjustments in the strategy of control in anticipation of a change in the loading conditions. We used such short sequences of unloaded trials for two reasons. First, to minimize the chances for the subject to realize that such trials could happen with a 50% probability. Second, to avoid fatigue. Avoiding fatigue was also the main reason why we used the 50:50% ratio of unperturbed and unloaded trials, not a less frequent presentation of unloaded trials, for example 20:80%, which could have an advantage of preventing changes in the lifting strategy as compared to the preceding trials without any unexpected events.

Another relatively artificial manipulation was setting a target pressing force prior to lifting the object. This could potentially have an effect on the control of the lifting phase. We used this particular experimental design to be able to quantify finger coordination (synergies) prior to the lift-off, which would be impossible to do if the fingers only touched the sensors producing effectively zero forces.

As in several earlier studies (e.g., Asatryan and Feldman 1965; Latash 1994), we relied on the subjects' ability “not to intervene” when the external conditions changed. In earlier studies, this assumption was tested by additional control tests in which the timing and spatial gradients of unloading were varied, yielding invariant torque–angle characteristics (Latash and Gottlieb 1991, 1992; Feldman and Levin 1995). These tests were difficult to conduct in the present study. However, we would like to note that the reproducibility of the subjects' behavior in the unloaded trials and its compatibility with the predictions formulated assuming non-intervention offer indirect support for the assumption that the subjects “did not intervene”.

Acknowledgments

Supported in part by NIH Grants AG-018751, NS-035032, and AR-048563.

References

Adamovich S, Archambault PS, Ghafouri M, Levin MF, Poizner H, Feldman AG. Hand trajectory invariance in reaching movements involving the trunk. Exp Brain Res 2001;138:288–303. [PubMed: 11460767]

Aoki T, Niu X, Latash ML, Zatsiorsky VM. Effects of friction at the digit-object interface on the digit forces in multi-finger prehension. Exp Brain Res 2006;172:425–438. [PubMed: 16496136]

Arbib, MA.; Iberall, T.; Lyons, D. Coordinated control programs for movements of the hand. In: Goodwin, AW.; Darian-Smith, I., editors. Hand function and the neocortex. Springer; Berlin: 1985. p. 111-129.

Asatryan DG, Feldman AG. Functional tuning of the nervous system with control of movements or maintenance of a steady posture. I. Mechanographic analysis of the work of the limb on execution of a postural task. Biophysics 1965;10:925–935.

Feldman AG. Functional tuning of the nervous system with control of movement or maintenance of a steady posture. II. Controllable parameters of the muscle. Biophysics 1966;11:565–578.

Feldman AG, Latash ML. Testing hypotheses and the advancement of science: Recent attempts to falsify the equilibrium-point hypothesis. Exp Brain Res 2005;161:91–103. [PubMed: 15490137]

Feldman AG, Levin MF. Positional frames of reference in motor control: their origin and use. Behav Brain Sci 1995;18:723–806.

Feldman AG, Levin MF. The equilibrium-point hypothesis—past, present and future. Adv Exp Med Biol 2009;629:699–726. [PubMed: 19227529]

Flanagan JR, Burstedt MK, Johansson RS. Control of fingertip forces in multidigit manipulation. J Neurophysiol 1999;81:1706–1717. [PubMed: 10200206]

Flanagan JR, Bowman MC, Johansson RS. Control strategies in object manipulation tasks. Curr Opin Neurobiol 2006;16:650–659. [PubMed: 17084619]

Friedman J, Flash T. Task-dependent selection of grasp kinematics and stiffness in human object manipulation. Cortex 2007;43:444–460. [PubMed: 17533767]

Gorniak SL, Zatsiorsky VM, Latash ML. Hierarchies of synergies: an example of the two-hand, multi-finger tasks. Exp Brain Res 2007a;179:167–180. [PubMed: 17103206]

Gorniak SL, Zatsiorsky VM, Latash ML. Emerging and disappearing synergies in a hierarchically controlled system. Exp Brain Res 2007b;183:259–270. [PubMed: 17703288]

Gorniak SL, Zatsiorsky VM, Latash ML. Hierarchical control of static prehension: II. Multi-digit synergies. Exp Brain Res 2009;194:1–15. [PubMed: 19048236]

Gysin P, Kaminski TR, Gordon AM. Coordination of fingertip forces in object transport during locomotion. Exp Brain Res 2003;149:371–379. [PubMed: 12632239]

Hajian AZ, Howe RD. Identification of the mechanical impedance at the human finger tip. J Biomech Eng T ASME 1997;119:109–114.

Hinder MR, Milner TE. The case for an internal dynamics model versus equilibrium point control in human movement. J Physiol 2003;549:953–963. [PubMed: 12717002]

Hogan N. The mechanics of multi-joint posture and movement control. Biol Cybern 1985;52:315–331. [PubMed: 4052499]

Iberall, T. The nature of human prehension: three dexterous hands in one. Proceedings of 1987 IEEE international conference robotics automation; Raleigh, NC. 1987. p. 396-401.

Johansson, RS. Sensory control of dexterous manipulation in humans. In: Wing, A.; Haggard, P.; Flanagan, R., editors. Hand and brain. Academic Press; San Diego: 1996. p. 381-414.

Johansson RS, Westling G. Roles of glabrous skin receptors and sensorimotor memory in automatic control of precision grip when lifting rougher or more slippery objects. Exp Brain Res 1984;56:550–564. [PubMed: 6499981]

Kang N, Shinohara M, Zatsiorsky VM, Latash ML. Learning multi-finger synergies: an uncontrolled manifold analysis. Exp Brain Res 2004;157:336–350. [PubMed: 15042264]

Kao I, Cutkosky MR, Johansson RS. Robotic stiffness control and calibration as applied to human grasping tasks. IEEE Trans Rob Autom 1997;13:557–566.

Kluzik J, Diedrichsen J, Shadmehr R, Bastian AJ. Reach adaptation: what determines whether we learn an internal model of the tool or adapt the model of our arm? J Neurophysiol 2008;100:1455–1464. [PubMed: 18596187]

Kugler, PN.; Turvey, MT. Information, natural law, and the self-assembly of rhythmic movement. Erlbaum; Hillsdale, NJ: 1987.

Latash ML. Reconstruction of equilibrium trajectories and joint stiffness patterns during single-joint voluntary movements under different instructions. Biol Cybern 1994;71:441–450. [PubMed: 7993931]

Latash, ML. Synergy. Oxford University Press; New York: 2008.

Latash ML, Gottlieb GL. Compliant characteristics of single joints: preservation of equifinality with phasic reactions. Biol Cybern 1990;62:331–336. [PubMed: 2310787]

Latash ML, Gottlieb GL. Reconstruction of elbow joint compliant characteristics during fast and slow voluntary movements. Neuroscience 1991;43:697–712. [PubMed: 1922790]

Latash ML, Gottlieb GL. Virtual trajectories of single-joint movements performed under two basic strategies. Neuroscience 1992;47:357–365. [PubMed: 1641128]

Latash ML, Zatsiorsky VM. Joint stiffness: myth or reality? Hum Move Sci 1993;12:653–692.

Latash ML, Zatsiorsky VM. Multi-finger prehension: control of a redundant motor system. Adv Exp Med Biol 2009;629:597–618. [PubMed: 19227523]

Latash ML, Scholz JF, Danion F, Schöner G. Structure of motor variability in marginally redundant multi-finger force production tasks. Exp Brain Res 2001;141:153–165. [PubMed: 11713627]

Latash ML, Kang N, Patterson D. Finger coordination in persons with Down syndrome: atypical patterns of coordination and the effects of practice. Exp Brain Res 2002a;146:345–355. [PubMed: 12232691]

Latash ML, Scholz JP, Schöner G. Motor control strategies revealed in the structure of motor variability. Exer Sport Sci Rev 2002b;30:26–31.

Latash ML, Scholz JF, Danion F, Schöner G. Finger coordination during discrete and oscillatory force production tasks. Exp Brain Res 2002c;146:412–432.

Latash ML, Scholz JP, Schöner G. Toward a new theory of motor synergies. Mot Control 2007;11:275–307.

Li S, Danion F, Latash ML, Li ZM, Zatsiorsky VM. Bilateral deficit and symmetry in finger force production during two-hand multi-finger tasks. Exp Brain Res 2001;141:530–540. [PubMed: 11810146]

Loeve, M. Probability theory. Van Nostrand; New York: 1955.

Marsden CD, Merton RA, Morton HB, Rothwell JC, Traub MM. Reliability and efficacy of the long-latency stretch reflex in the human thumb. J Physiol 1981;316:47–60. [PubMed: 7320877]

Mason, MT.; Salisbury, JK. Robot hands and the mechanics of manipulation. The MIT Press; Cambridge: 1985.

Milner TE, Franklin DW. Characterization of multijoint finger stiffness dependence on finger posture and force direction. IEEE T Bio-med Eng 1998;45:1363–1375.

Niu X, Latash ML, Zatsiorsky VM. Prehension synergies in the grasps with complex friction patterns: local vs. synergic effects and the template control. J Neurophysiol 2007;98:16–28. [PubMed: 17493928]

Ostry DJ, Feldman AG. A critical evaluation of the force control hypothesis in motor control. Exp Brain Res 2003;153:275–288. [PubMed: 14610628]

Pilon JF, De Serres SJ, Feldman AG. Threshold position control of arm movement with anticipatory increase in grip force. Exp Brain Res 2007;181:49–67. [PubMed: 17340124]

Rossi E, Mitnitski A, Feldman AG. Sequential control signals determine arm and trunk contributions to hand transport during reaching in humans. J Physiol 2002;538:659–671. [PubMed: 11790827]

Santello M, Soechting JF. Force synergies for multifingered grasping. Exp Brain Res 2000;133:457–467. [PubMed: 10985681]

Schmidt RA, McGown C. Terminal accuracy of unexpected loaded rapid movements: evidence for a mass-spring mechanism in programming. J Mot Behav 1980;12:149–161. [PubMed: 15215060]

Scholz JP, Schöner G. The uncontrolled manifold concept: identifying control variables for a functional task. Exp Brain Res 1999;126:289–306. [PubMed: 10382616]

Scholz JP, Kang N, Patterson D, Latash ML. Uncontrolled manifold analysis of single trials during multi-finger force production by persons with and without Down syndrome. Exp Brain Res 2003;153:45–58. [PubMed: 12928761]

Shadmehr R, Mussa-Ivaldi FA. Adaptive representation of dynamics during learning of a motor task. J Neurosci 1994;5:3208–3224. [PubMed: 8182467]

Shadmehr, R.; Wise, SP. The computational neurobiology of reaching and pointing. MIT Press; Cambridge: 2005.

Shim JK, Latash ML, Zatsiorsky VM. Prehension synergies in three dimensions. J Neurophysiol 2005;93:766–776. [PubMed: 15456799]

Traub MM, Rothwell JC, Marsden CD. A grab reflex in the human hand. Brain 1980;103:869–884. [PubMed: 7437893]

Van Doren CL. Grasp stiffness as a function of grasp force and finger span. Mot Control 1998;2:352–378.

Wolpert DM, Miall RC, Kawato M. Internal models in the cerebellum. Trends Cogn Sci 1998;2:338–347.

Yang JF, Scholz JP, Latash ML. The role of kinematic redundancy in adaptation of reaching. Exp Brain Res 2007;176:54–69. [PubMed: 16874517]

Zatsiorsky, VM. Kinetics of human movement. Human Kinetics; Champaign: 2002.

Zatsiorsky VM, Latash ML. Prehension synergies. Exer Sport Sci Rev 2004;32:75–80.

Zatsiorsky VM, Latash ML. Multi-finger prehension: an overview. J Motor Behav 2008;40:446–476.

Zatsiorsky VM, Li ZM, Latash ML. Enslaving effects in multi-finger force production. Exp Brain Res 2000;131:187–195. [PubMed: 10766271]

Zhang W, Scholz JP, Zatsiorsky VM, Latash ML. What do synergies do? Effects of secondary constraints on multi-digit synergies in accurate force-production tasks. J Neurophysiol 2008;99:500–513. [PubMed: 18046000]

Zhang W, Olafsdottir HB, Zatsiorsky VM, Latash ML. Mechanical analysis and hierarchies of multi-digit synergies during accurate object rotation. Mot Control 2009;13:251–279.

NIH-PA Author Manuscript

NIH-PA Author Manuscript

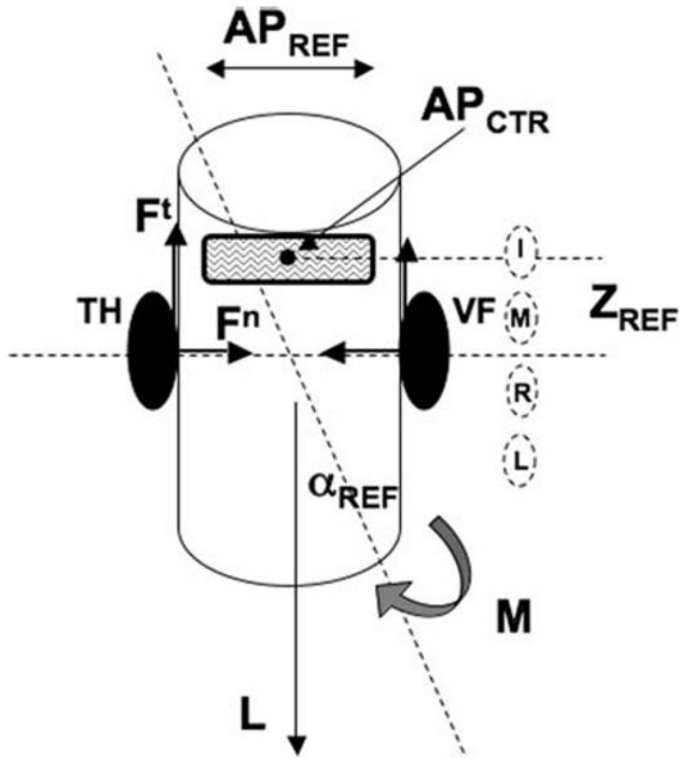

Fig. 1.
An illustration of a thumb–virtual finger (*TH–VF*) grip in a planar case. An external load and moment of force (*L* and *M*) act on the hand-held object. The controller sets a referent configuration, which leads to peripheral effects that may be described with four geometric parameters: The size and location of the referent aperture (AP_{REF} and AP_{CTR}), referent vertical position (Z_{REF}), and referent orientation (α_{REF}). Virtual finger produces force and moment of force equal to the sum of the forces and moments of force produced by the four individual fingers (*I* index, *M* middle, *R* ring, and *L* little)

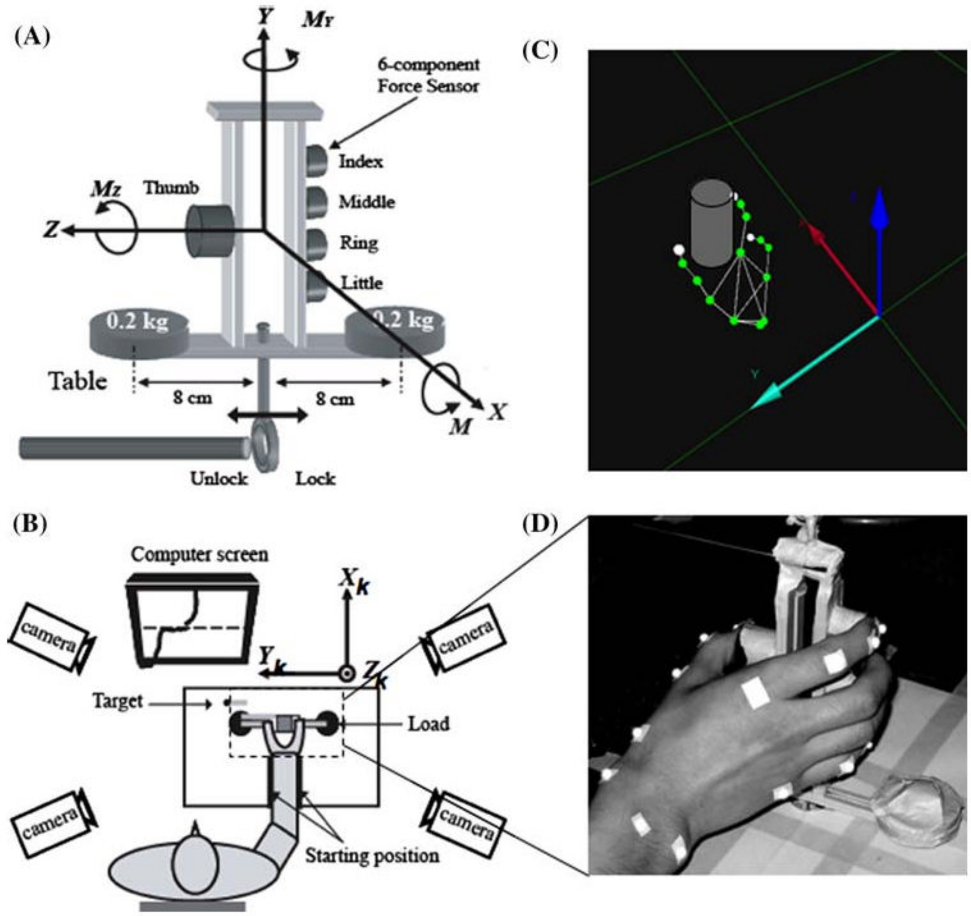

Fig. 2.

Experimental setup. **a** A schematic diagram of the aluminum handle; the force/moment sensors shown as *black* cylinders were attached to two vertical aluminum bars. The loads (0.21 kg) are shown as *black* cylinders attached to the long horizontal beam; *Left* (−0.15 Nm), *No* (0 Nm), and *Right* (0.15 Nm) external torque conditions. A lock system was attached to a metal loop and was secured with an eyehook directly underneath the table in the medio-lateral direction. **b** The approximate location of four cameras and the experimental table used for motion capture (*top view*; figure is not to scale). The monitor presented the target line and gave feedback about the level of force at the constant force phase before the hand movement. **c** The hand model in the starting position. **d** The starting hand posture together with marker locations on the hand and wrist; 15 consistently identifiable and palpable surface landmarks: fingertips (*FT*), distal interphalangeal (*DIP*), proximal interphalangeal (*PIP*), and metacarpophalangeal (*MCP*) or carpo-metacarpal (*CMC*) joints, wrist joints for radius and ulnar styloid, and the midpoint between two wrist markers. Note that there are two coordinates systems, *X*, *Y* and *Z* fixed relative to the handle, and X^k, Y^k and Z^k fixed relative to the laboratory

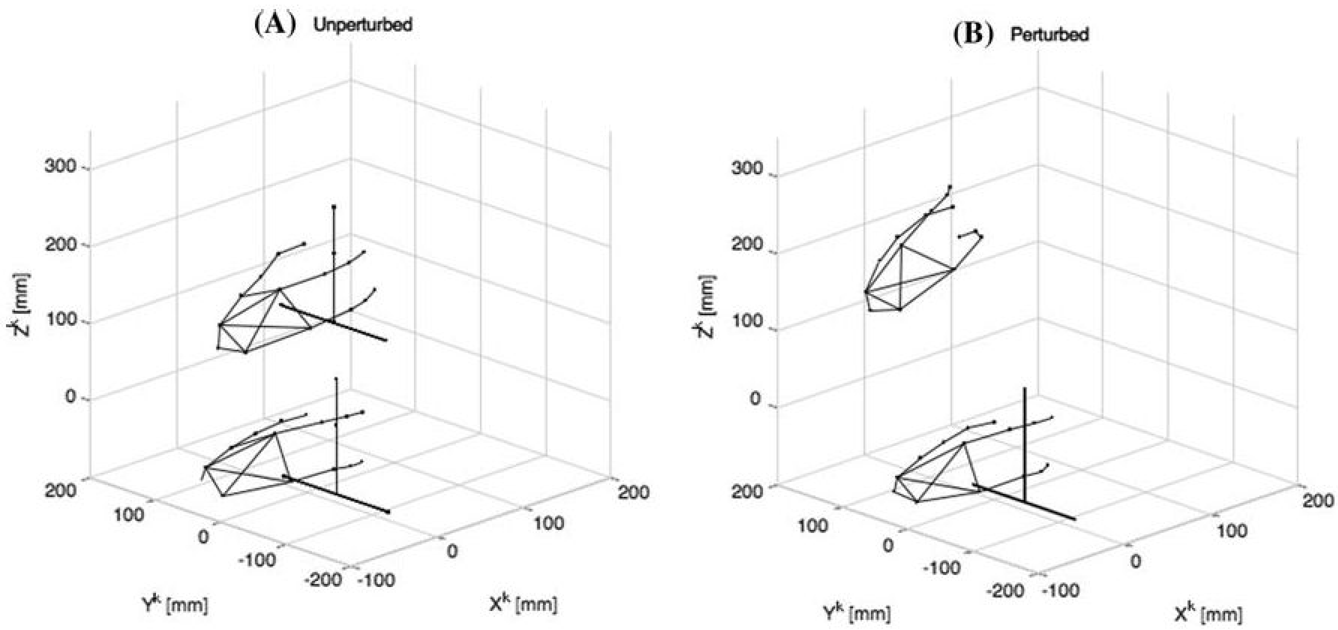

Fig. 3.
Initial and final 3D hand locations. **a** Shows the hand and the handle at the start position and at the final steady state position during a typical unperturbed movement. The handle is shown as an inverse T-shape. **b** Shows the hand position in a typical perturbed trial. The results presented are from the no external torque condition

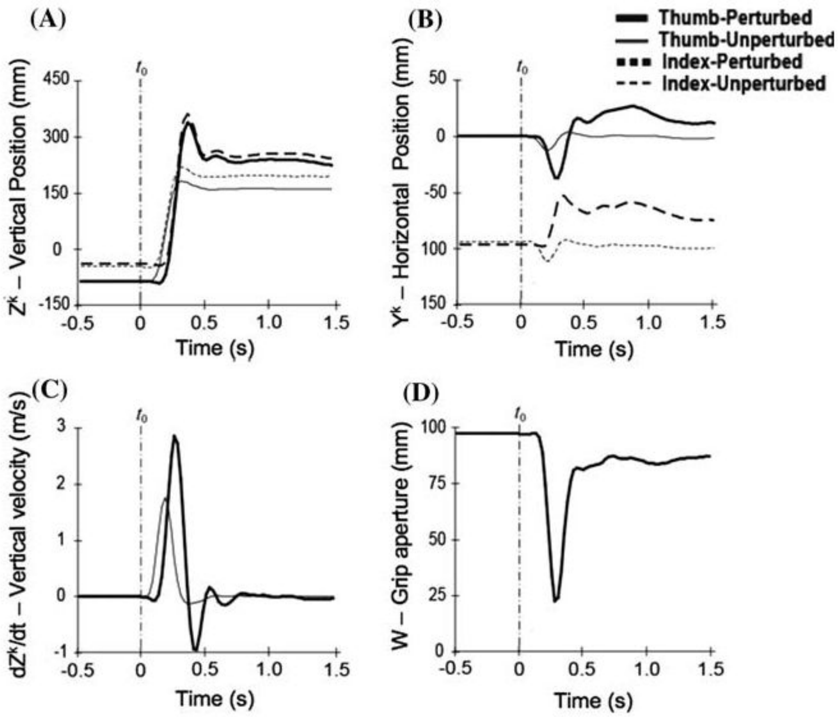

Fig. 4.

Kinematic patterns for the average of three perturbed (*thick lines*) and three unperturbed (*thin lines*) trials performed by a typical subject. **a** The vertical position (Z^k) of the thumb (*thick solid lines*) and index (*dashed lines*) fingertips. **b** The horizontal (Y^k) position of the thumb and index fingertips. **c** The vertical velocity (dZ^k/dt) of the thumb. **d** The grip aperture (W) of the thumb and index fingers, for a perturbed trial. The onset (t_0) of the movement was defined by 5% of the peak derivative of grip force. The data are for the zero external torque condition

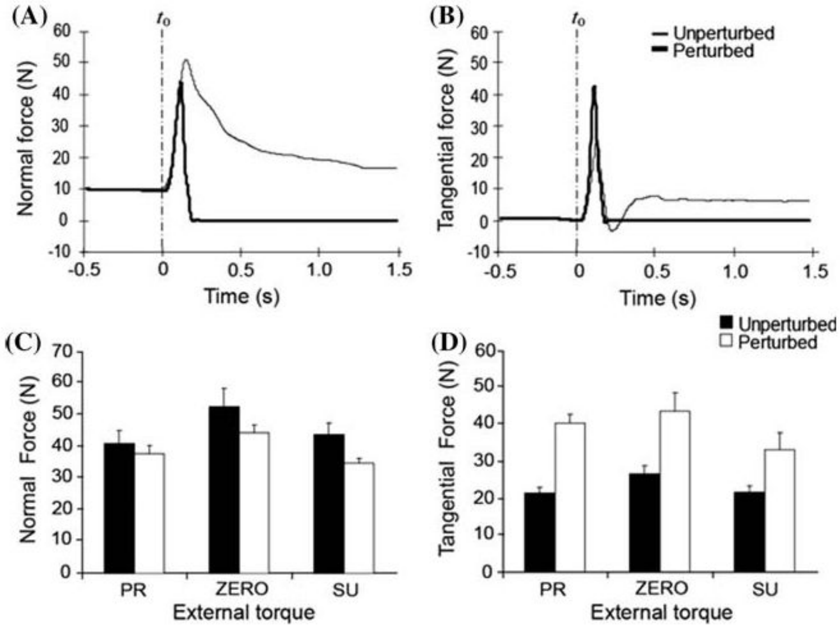

Fig. 5.

a The total normal (grip) force of the four fingers (IMRL) and **b** tangential (load) forces as a function of time in the perturbed (*thick lines*) and unperturbed (*thin lines*) trials. The movement started at time $t = 0$ s (t_0). **c** Peak normal and **d** tangential force in the unperturbed (*black bars*) and perturbed (*white bars*) conditions. The data was averaged over 12 trials (unperturbed) and two trials (perturbed) for each subject and further averaged across all subjects. Data averaged across subjects are shown with standard error bars

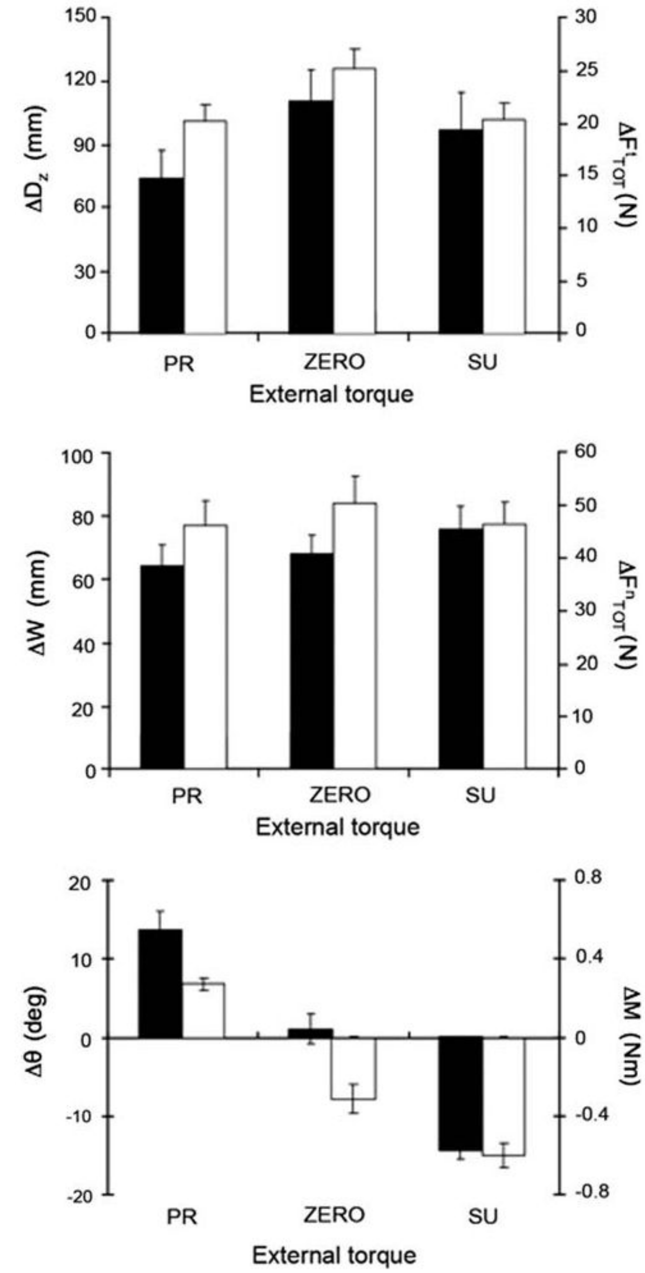

Fig. 6.

a Changes of path height ΔD_Z (*black bars*) and peak tangential forces $\Delta F^{t}_{\mathrm{TOT}}$ (*white bars*). Both quantities are higher in the presence of a ZERO external torque as compared the PR and SU conditions. **b** Changes in aperture ΔW (*black bars*) and grip forces $\Delta F^{n}_{\mathrm{TOT}}$ (*white bars*). **c** Changes in hand rotation $\Delta\theta$ (*black bars*) and moment about the *x*-axis ΔM (*white bars*). Data are averaged across subjects, standard error bars are shown

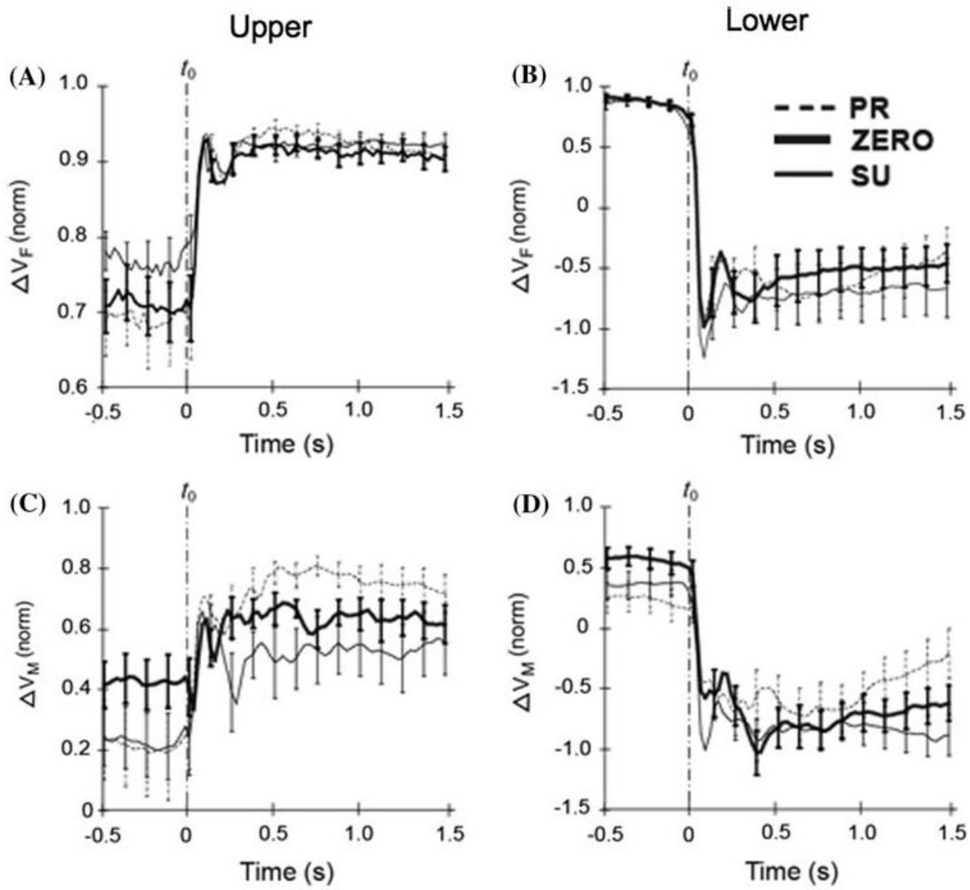

Fig. 7.

Indices of digit force covariation, $\Delta V_F(t)$, at the upper (**a**) and lower (**b**) levels. Indices of digit moment of force covariation, $\Delta V_M(t)$, at the upper (**c**) and lower (**d**) levels in the unperturbed condition. The onset (*dashed vertical lines*) of hand lifting was at time $t = 0$ s (t_0). Different lines show data during lifting the hand in different external moment conditions, PR (*dashed line*), ZERO (*thick solid line*), and SU (*solid line*)